Soft Ferromagnetic Microwires with Excellent Inductive Heating Properties for Clinical Hyperthermia Applications

by

Rupin Singh

A honor thesis submitted in partial fulfillment
of the requirements for the degree of
Bachelor of Science in Biomedical Sciences
The College of Arts and Sciences
University of South Florida

Supervisor: Manh-Huong Phan, Ph.D.

Date of Approval:
April 22, 2015

Keywords: magnetics, microwires, hyperthermia, biomedicine

ACKNOWLEDGEMENT

I would first like to thank those it my thesis committee, Dr. Manh-Huong Phan, Dr. Jaganath Devkota, and Dr, Javier Alonso, for their supervision, continuous help at all hours of day, and their fantastic instruction that allowed me to be introduced to the field of magnetic particles. They have opened my eyes to the wide applications that can present themselves in material sciences. Additionally, I will also like to thank Dr. Pritish Mukherjee who recommended me and introduced me to Dr. Phan for the first time. Without his help, I would never have been able to learn and experience what I have over the past two semesters including meeting many inspiring individuals. I would also like to thank Dr. Hari Srikanth for providing me access to some of the facilities at USF in which I could conduct my research. Finally, I would like to thank the rest of the Functional Materials Laboratory Group at USF for their ability to assist me anyway they could.

Research at USF Physics was supported by the Florida Cluster for Advanced Smart Sensor Technologies (FCASST) and by the United States Army (Grant No. W81XWH1020101/3349).

TABLE OF CONTENTS

ABSTRACT

Growing interest in the use of magnetic particles for biomedical applications has led researchers to investigate a multitude of treatment possibilities to use clinical hyperthermia for cancer therapy. Glass-coated microwires have been shown to be easy to produce, control, and insulate for biocompatibility along with their outstanding magnetic properties (large saturation magnetization and large shape anisotropy). This thesis provides the first exploration of the radio frequency alternating field responses of magnetically soft Co-rich glass-coated microwires for possible applications in clinical hyperthermia. We have performed a systematic study of the influence of wire morphology on heating efficiency of the hyperthermia treatment. Synthesized by the Taylor-Ulitovsky method, these glass-coated microwires, CoMnSiB and CoFeSiBCrNi, have shown high magnetization saturation and low coercivity based on their magnetization measurements. For the magnetic hyperthermia treatment, the glass-coated microwires were placed in a small glass vial in an alternating magnetic field to measure heat loss and analyze their specific absorption rate (SAR). The shape effects revealed in this study include that increasing core thickness and decreasing glass thickness show a substantive increase in SAR. Additionally, when testing in an alternating magnetic field parallel and perpendicular to the domain axis of the wire, it was determined that a parallel orientation provides the best heat loss. Interactions between multiple microwires demonstrated positive effects on the SAR value as tightly packed microwires yielded better heat loss. Overall, our study demonstrates that soft ferromagnetic glass-coated microwires continue to show promising applications for hyperthermia as we better control microwire morphology and their magnetic softness.

1. INTRODUCTION

1.1 Overview

Although the spread of cancer continues to decline, down twenty-two percent in the US over the past two decades [1], it is still the leading cause of death worldwide, accounting for 8.2 million deaths in 2012 alone [2]. Therefore, there is a pressing need to improve and develop cancer treatments to continue to improve survival rates and patient well-being. The unregulated growth of cells associated with cancer normally causes a low pH and hypoxia to occur in the tumors and surrounding tissue [3]. These are not ideal conditions for radiation therapy or cytotoxic drugs as their delivery is severely hindered to a much lower concentration. Additional treatment cannot be done without doing harm to the patient as well, such as inducing high levels of radiation to patients. Magnetic hyperthermia is one alternative avenue researchers are investigating to improve cancer treatments success rates and reduce patient discomfort.

The use of magnetic nanoparticles in medicine is rapidly growing due to their variability in size, shape, coating, and ability to perform noninvasive procedures. They can be used as a means to monitor chemical and biological systems as magnetic sensors, to perform deep tissue penetration for drug delivery, magnetic cell separation and purification, magnetic resonance imaging contrast enhancement, purification, bioassay, gene transfer, and hyperthermia of cancerous tissue [4,5]. For magnetic hyperthermia, however, magnetic nanoparticles present some limitations. It has been reported that if the nanoparticles are injected intravenously they tend to be covered with proteins (opsonized), thus encouraging their phagocytosis. The

nanoparticles can also be recognized as “foreign bodies” and eliminated by the reticuloendothelial system [6]. To avoid the action of the immune system, there is an increasing need for controlling their size, surface functionality, aggregation, and size distribution. It has also been reported that once the treatment is finished, the nanoparticles tend to accumulate in the liver and spleen, with unwanted toxic effects [7]. Therefore, alternative materials have recently been proposed. In particular, the use of ferromagnetic implants or needles for magnetic hyperthermia, which was recognized a few decades ago as a promising approach [8], has renewed interest in the scientific community [9].

Soft ferromagnetic glass-coated microwires (GCMWs) of 5 – 150 μm diameter have emerged as one of the most promising soft magnetic materials, owing to their outstanding magnetic properties (e.g. magnetic bistability, giant magneto-impedance (GMI) effect, fast domain wall propagation, and Hopkinson effect) for a wide variety of applications in magnetic sensors, microelectronics, security, and biomedical engineering [10]. The continuous microwires up to few kilometers can easily be fabricated from one gram of master alloy [11]. The extremely large saturation magnetization and shape anisotropy coupled with their strong responses to AC magnetic fields suggest that the GCMWs can be a promising candidate for use in magnetic hyperthermia. The glass coating itself provides electrical insulation and also improves biocompatibility [10]. In this thesis, we aim to explore radio frequency field responses of magnetically soft Co-rich glass-coated microwires for clinical hyperthermia applications while investigating the effect of multiple variables of interest including metal composition, core diameter, glass-coating diameter, orientation, and multiple microwire interactions.

1.2 Magnetic Hyperthermia

Magnetic hyperthermia mediated by magnetic structures is based on raising the temperature of a localized tumor area in order to impede or kill malignant cells within the body. Normally performed synergistically with more common treatments such as radiotherapy and chemotherapy [12], hyperthermia is usually carried out at defined local hyperthermic levels, i.e. temperatures around 42-45°C. In this temperature range, hyperthermia does not induce cell death, only disrupts cellular metabolism and impede cancer proliferation. On the other hand, thermoablation relies on the use of hyperthermia in order to induce rapid cell death at temperatures above 50 °C. At this point, vital proteins of the cancer cell become damaged and the cell membrane partially dissolves into the aqueous solution surrounding it [12]. This technique has a high risk of severe or persistent side effects and can potentially lead to dire consequences depending on the size of the target region Thermoablation may be feasible for some cancer morphologies but as long as one can assure side-effects are reduced to reasonable levels.

The basic magnetic hyperthermia involves injecting a ferrofluid, i.e. a stable colloidal dispersion of iron magnetic particles in an aqueous media, or inserting wires into the cancerous body [6]. The cancerous location in the body is remotely targeted from active or passive external magnetic field gradients and then subsequently an external alternating magnetic field (usually between a few kHz to 1 MHz) is added to the localized site to heat cancer cells. Contemporary research demonstrates an ability to increase specificity and reliability of magnetic structures for hyperthermia by altering delivery methods, synthesis methods, optimization of their coating, optimization of their size to heat delivered ratio, and attempts to reduce the indirect heating of healthy tissue [13].

The use of fine magnetic particles for magnetic hyperthermia has not only been known for decades but also has been an active field of research for over 50 years. Early research by Dr. Gilchrist was first done in 1965 to kill lymph node metastases. It was an attempt to treat colon cancer by applying an alternating magnetic field of 55 kHz to the ferrite nanoparticles of size 100-500 nm. Gilchrist demonstrated that by applying an external AC field, the nanoparticles gave rise to heat losses proportional to the frequency of the field [14]. The targeted tissue is mainly heated by two physical phenomena, eddy currents and magnetic hysteresis [3]. The eddy currents, the primary heat source in typical bulk magnetic structures, oppose the applied magnetic field and by the Joule effect, produce heating [15]. In ferromagnetic materials, such as magnetic particles, the heating is mainly due to magnetic hysteresis losses originated by the lag between the magnetic moments of the particles and the oscillating magnetic field [16]. The advantages of using modern hyperthermia systems are huge and all are important to the patient's safety and well-being.

In addition to the use of fine magnetic particles, ferromagnetic implants, i.e. needles or micro/nanowires, have been developed for enhanced hyperthermia. It has recently been reported that the magnetic needles show even higher heating efficiency rates, as compared to iron oxide nanoparticles [17]. Therefore, it is more important than ever to be able to control the spatial distribution of heat to be both very strong and homogenous. Ferromagnetic microwires have demonstrated the ability to be self-regulated because of their tailored Curie temperatures [18]. Some materials proposed outside microwires include Fe-based amorphous ribbons, biocompatible Mg-Fe based ceramics, and nickel-zinc nanoparticles [18].

1.3 Magnetic Nanostructures

Bulk ferromagnetic, ferrimagnetic, and antiferromagnetic materials have magnetic domains in which their dipoles align spontaneously due to the exchange interaction. Paramagnetic and diamagnetic materials, on the other hand, do not have permanent magnetic domains with spontaneously aligning dipoles but have dipoles that can respond to an applied external field. Each of these magnetic materials are distinguished based on their dipole moment orientation, i.e. paramagnetic materials form dipoles along the axis of the field while diamagnetic materials form dipoles against the axis of the magnetic field. This phenomenon can be investigated by measuring their magnetization in changing magnetic field strengths. Where paramagnetic materials demonstrate a positive and linear behavior to an increasing magnetic field H, the magnetization M of a ferromagnetic material, characterized with a large susceptibility (M to H ratio), exhibits a non-linear relationship and even retains magnetization memory after the magnetic field is removed [6]. This causes a hysteresis in the M(H) loop of the ferromagnetic material.

Magnetic nanoparticles (MNPs) present different magnetic behaviors depending on their diameters, compositions, and coatings. When smaller than their critical diameter, each MNP is considered to have only one large magnetic moment, also known as a "superspin" [19]. Here, domain formation is no longer energetically favorable [3]. It is at this nanoscale that ferromagnetic and ferrimagnetic materials can demonstrate this superparamagnetic behavior, i.e. spontaneous domain spin reversals under the influence of temperature. In this state, their magnetic susceptibility is very high, much higher than normal paramagnets [3]. Figure 1.1 shows the variation in coercive field (H_c) as the particle size is decreased to the nanoscale, along with the magnetic loops or the M(H) curves representing three different regimes: multidomain, single

domain, and superparamagnetism. In case of superparamagnetism, the M(H) curve becomes nonlinear even at low magnetic fields. The time between spin reversals is given by the Néel relaxation time expression and will cause micro or nanoparticles to exhibit zero magnetization unless under the influence of an external magnetic field. Each material has a different attempt time for spin reversal, typically between 10^{-9} and 10^{-10} seconds. There is a critical temperature, known as the blocking temperature, below which the magnetic material will not remain superparamagnetic and it is dependent on the anisotropy energy and volume of the material [20]. For a spherical material, we can define the diameter of the material that it must be to become superparamagnetic based on their anisotropy. The critical diameter for most materials has been demonstrated to be approximately 100 nm [21].

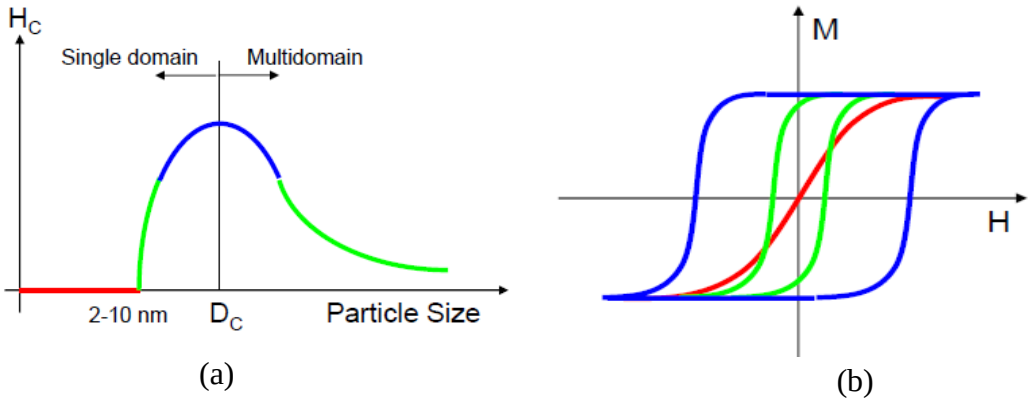

(a) (b)

Figure 1.1 (a) Dependence of coercive field (H_c) on particle size and the M(H) loops of the particle samples corresponding to the multidomain, single domain, and superparamagnetic regimes [22]. Unlike a ferromagnetic material (blue or green), superparamagnetic nanoparticles show zero coercivity and zero remanent magnetization (red).

1.4 Soft Ferromagnetic Glass-Coated Microwires

Glass-coated microwires are a composite material that consists of a metallic nucleus and a glass-coating. The metallic nucleus ranges from 100 nm to 50 μm in diameter while the glass-coated thickness ranges from 2 to 20 μm [23]. As a result of their amorphous structure, glass-coated microwires are characterized by low magnetic anisotropy. Their magnetic properties are mainly dictated by magnetoelastic and shape anisotropy. Overall, amorphous microwires possess large shape anisotropy, magnetoelastic anisotropy, and ultra-soft magnetic properties such as a high permeability, large saturation magnetization (M_s), and low magnetic field anisotropy (H_s). They have a characteristic core/shell structure that dictates their magnetic properties.

Soft ferromagnetic amorphous glass-coated microwires are particularly interesting because thus far their research has been limited to other applications such as GMI and microwave sensing [16]. Their applications in hyperthermia could open a new avenue for biocompatible hyperthermic treatments without the need for carefully crafted magnetic nanoparticles and nanowires. Their commercial availability and cheap/efficient preparation increase the access institutions to have for the treatment which can ultimately lower the cost of care for both the health care provider and the patient. During the production of these amorphous glass-coated microwires, a combination of axial and tensile radial stresses affects their magnetic properties [23]. This is usually dependent on the metallic composition of the alloy causing them to be divided into three groups, positive magnetostrictive, negative magnetostrictive, and low magnetostrictive.

Positive magnetostrictive wires are Fe-rich alloys, negative magnetostrictive wires are Co-rich (mainly CoSiB-based microwires), and low magnetostrictive wires are usually CoFeSiB-based microwires with 3-5% Fe-based. The domain structures for each of these are shown in

Figure 1.2. It can be seen that amorphous magnetic microwires form a core-shell type of domain structure but in different patterns and orientations depending on their magnetostriction. The positive magnetostrictive microwires have longitudinal core domains oriented along the wire axis while the shell forms radial domains (Figure 1.2(a)). Due to this domain structure, the magnetization process propagates along the entire microwire in a single Barkhausen jump, forming a rectangular-shaped magnetic hysteresis loop. Due to this, they are easy to detect and are commonly used in the construction of small sensors. Negative magnetostrictive alloys form circular domains perpendicular to the domain axis (Figure 1.2(b)). Therefore, magnetization in the axial direction along the microwire causes rotations of magnetic moments inside the domains so their magnetization is proportional to the applied magnetic field.

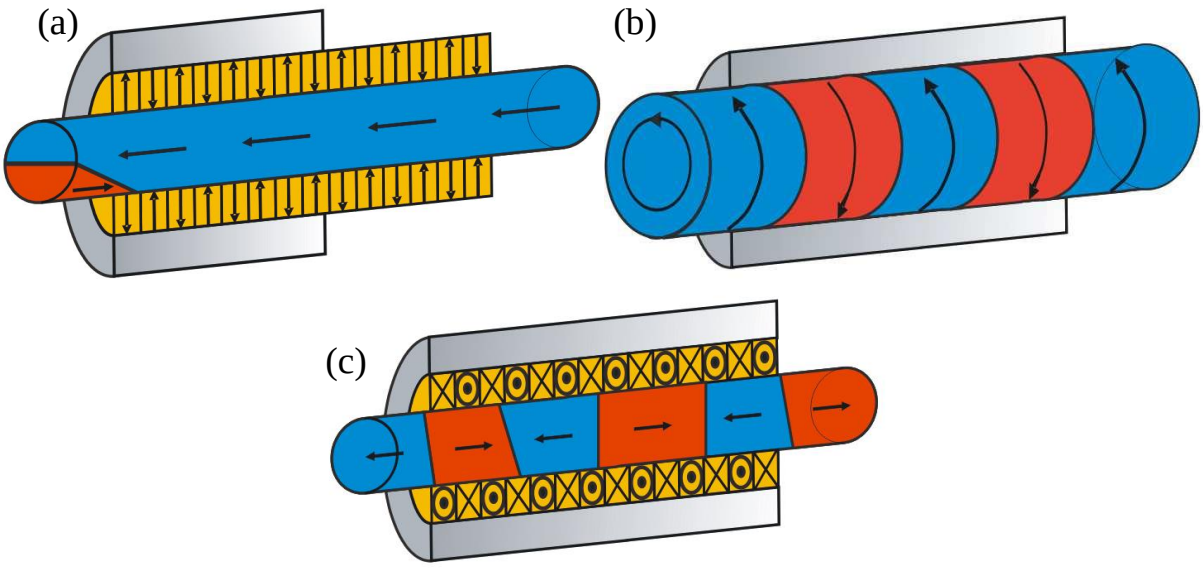

Figure 1.2 Schematic domain structures of glass-coated microwires with (a) positive magnetostriction, (b) negative magnetostriction, and (c) low magnetostriction [23].

The hysteresis loops of negative magnetostrictive microwires are small due to the perpendicular alignment of the magnetic moments in an external magnetic field. The low magnetostrictive alloys have less defined domain structures, as visible in Figure 1.2(c), but still show circular domains below the surface of the nucleus and an axial domain in the center of the wire [15]. These nearly zero magnetostrictive microwires demonstrate normal-shaped hysteresis loops due to the balance between the magnetoelastic and magnetostatic energies.

To exhibit an excellent hyperthermic effect, microwires should have extremely soft magnetic properties, large but well defined anisotropy, and negative magnetostriction [24]. Considering this, we have selected the two following materials for our study, CoMnSiB and CoFeSiBCrNi, both of them exhibiting negative magnetostriction. Once an external magnetic field is applied, the effects of orientation to the magnetic field and interactions between different microwires have been tested to see if the domain structures have a positive or negative effect on the field's effectiveness. In addition, we have also investigated how the thickness of the glass-coating and the core diameter affect the hyperthermia efficiency of these microwires. Finally, the effect of having multiple microwires interacting among each other has been analyzed.

2. EXPERIMENTAL

In this section, we discuss a brief description of the experimental materials and methods used in this thesis. We first present the fabrication technique of the amorphous microwires. Then, we provide an overview of the characterization techniques, how the magnetic properties of the microwires are measured, and descriptions of the hyperthermia measurement setup in the lab.

2.1 Fabrication of Microwires

Amorphous metallic wires are generally made in five different methods: melt spinning, in-rotating water spinning, Taylor-wire process, glass-coated melt spinning, and electrodeposition. Melt spinning is the most widely used technique and the basis for some of the other techniques. It can create microwires with diameters from 1 μm to 300 μm. The main process is a pressure ejection of melt stream through an outlet and into a cooling fluid followed by rapid solidification of this stream before it breaks into droplets, i.e. rapid quenching. Three conditions must be met in order for this to work: the solidification must occur within the "stability" distance from the ejection point, the cooling fluid used must be of low viscosity and surface tension, and that there is stable and non-turbulent flow of the cooling liquid at high viscosities [25]. By absorbing heat from the molten mass so fast, the mass becomes a non-crystalline alloy, i.e. an amorphous alloy. This basic process can then be modified and advanced at various steps to allow for addition of a glassy coat, changes in physical and magnetic properties, and changes to the shape and dimensions of the product to fulfill a different purpose such as amorphous ribbons [25].

Electrodeposition, on the other hand, is a more recent method used to create uniform wires consisting of a non-magnetic conducting inner core, such as Copper-based, and a magnetic outer shell, such as made with FeNi. It involves the use of electrolytic baths that the metallic wire passes through to form two successive plating layers with rotating rollers to smooth out the surfaces [26]. The inner core is usually started at around 20 μm while the outer core forms a thickness between 2 – 7 μm [27]. The composition ratio and magnetic field can be controlled to determine the final properties of the wire.

The Co-rich amorphous glass-coated microwires used in this experiment were fabricated by the Taylor-Ulitovsky technique, a more advanced form of the normal Taylor-wire spinning synthesis. They were provided by MicroFir Tehnologii Industriale, Moldova. The Taylor-wire process was first introduced by G. F. Taylor in 1924 to produce fine microwires with a uniform cross section. He combined 13 pure metals and numerous alloys of these metals into a single amorphous wire. Essentially, he filled a Pyrex glass tube with metal from which the wire is drawn. It is placed in a heated cylinder of flame and is drawn as fine as desired [28]. A schematic of the method from Taylor's original paper is shown in Figure 2.1 below.

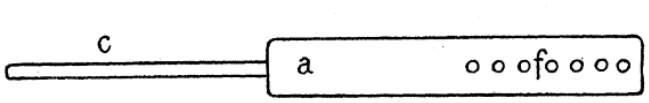

Figure 2.1 G.F. Taylor's original diagram demonstrating the Taylor-technique for microwire synthesis [29].

Modern methods involve the use of a high frequency inductive coil to melt the alloys. The casted wire is placed on a rotating metal disk with a speed about 5 m/s to cool the wire down at a rate of approximate 10^5 K/s [25]. Long microwires with 1-100 μm can be formed [28].

The modified Taylor-Ulitovsky, also known as the glass-coated melt spinning technique, allows for continuous production of the amorphous wire but inside a glass coat by changing the cooling rate. It was developed by Ultivosky, Wiesner, and Schneider [30-31]. Rather than using a rotating disk, the melts are fed into a stream of cold water. The glass coat prevents direct contact between the melts and the water. This method, however, requires precautions. This includes correctly evaluating the rate of oxidation of the melted alloy and choosing the correct glass that it is softened between the melting and solidifying temperatures so it should not react with the metal. If it reacts, the glass will contaminate the microwires.

2.2 Structural Characterization

2.2.1 Composition, Physical Properties, and Dimensions

The glass-coated microwires in this lab come in two different alloy compositions which we will describe using their manufacturer labels, 1675 and 1597. Both are soft magnetic amorphous Co-rich microwires with complex magnetic characteristics. The composition of each microwire is outlined in Tables 2.1 and 2.2. The tables show that alloy number 1675 is $Co_{68}B_{15}Si_{10}Mn_7$ and alloy number 1597 is $Co_{64.63}B_{16}Si_{11}Fe_{4.97}Cr_{3.4}Ni_{0.02}$.

Metal	**Mass %**	**Atomic %**
Co	82.90	68.00
B	3.40	15.00
Si	5.80	10.00
Mn	7.90	7.00

Table 2.1 Composition of Alloy Number 1675.

Metal	Mass %	Atomic %
Fe	5.85	4.97
Co	80.26	64.63
B	3.62	16.00
Si	6.48	11.00
Cr	3.76	3.40
Ni	0.02	0.02

Table 2.2 Composition of Alloy Number 1597.

These microwires have high curie temperatures and crystallization temperatures, making them ideal for hyperthermia because of their ability to maintain their magnetization properties at high temperatures. For example the curie temperature of 1597 is 250 °C and the crystallization temperature is 520 °C. The density of each of these microwire alloys was estimated based on their mass percent. The estimation is normally only useful for crystalline alloys rather than amorphous ones but provides good estimation of the true density without physically removing the glass coating and measuring the densities in the lab. The formula used to estimate the density is shown below:

$$\frac{1}{D_f} = \sum_{1}^{n} \frac{x_n}{D_n}$$

Where D_f is the final density of the allow, n is the number of metals that make up the allow, x is the mass fraction of that metal in the alloy, and D is the density of the pure metal. The estimated density of alloy number 1675 is 6.98 g/cm^3 and the estimated density of alloy number 1597 is 6.84 g/cm^3.

In addition to using two different alloys, wires of different core diameters and glass thicknesses were used to determine how each affects the inductive heating efficiency. As a side-

effect of the synthesis technique, the microwires do not have the same diameter across the entire length of the wire. The average diameter, however, has been calculated and is used as the measuring point. Each thickness was given a number label that corresponds to its alloy. #1-4 correspond to alloy number 1675, while #5-12 correspond to alloy number 1597. The average diameters of the total, core, and glass coating for each microwire tested are summarized in Table 2.3.

Table 2.3 Average thicknesses of the microwires.

Alloy and Label	Total thickness (μm)	Core thickness (μm)	Glass thickness (total – core) (μm)
1675-1	28.8	22.8	6.0
1675-2	20.2	12.9	7.3
1675-3	21.7	15.6	6.1
1675-4	32.5	25.3	7.2
1597-7	26.9	16.9	10.0
1597-8	18.2	12.7	5.5
1597-10	23.4	16.5	6.9
1597-11	22.7	16.7	6.0
1597-12	19.8	14.2	5.6

2.2.2 X-ray Diffraction

X-ray diffraction (XRD) is a popular technique to study the crystalline structure of materials by using Bragg's law of diffraction. Developed in 1913 by physicist Sir W.H. Bragg and his son, he tried to explain why cleavages at crystal faces reflect X-Ray beams at different angles of incidence and demonstrated the atomic structure of crystals [32]. Now, XRD is used to

study the structure of matter in all states, even at the subatomic level. Different crystallographic phases cause different angles to be reflected. This is described by Bragg's law:

$$2dsin\theta = n\lambda$$

Where d is the distance between atomic layers in the crystal, θ is the angle of incidence, λ is the wavelength of the X-ray incident on the crystal, and n is the order of diffraction in the direction of θ. From the intensities of all of the diffracted rays found in any direction, one gains information about crystal phase, size, and shape of the grains forming the material being analyzed.

In this experiment, a Bruker AXS D8 diffractometer at the University of South Florida (USF) Physics department with Cu K_α 1.5418 A was used in a θ - 2θ mode in order to get information about crystal phases of the Co-rich microwires. The XRD data gave us information about how amorphous the microwires used in this experiment truly are.

2.2.3 Scanning Electron Microscope

Scanning electron microscope (SEM) is an imaging technique for solid materials that uses a high-energy electron beam in a vacuum to reveal information about the external morphology, chemical composition, and crystalline structure and orientation [33]. An electron gun produces a beam of electrons that originates a variety of signals including X-rays, Auger electrons, primary backscattered electrons, and secondary electrons. Detectors collect all of the signals and process them to form a final image that can be viewed [33]. This technique is limited by only being able to describe surface features of conductive materials but can do so with a very high resolution because of the small wavelengths produced by reflecting electrons. All samples used in SEM must be dried from any moisture. In combination with other imaging techniques

such as Electron Backscatter Diffraction and Energy-Dispersive X-Ray Spectroscopy, SEM becomes a very powerful tool in the lab.

In this experiment, a JEOL JSM-6390LV SEM at USF Physics department was used to image the surface morphology of the Co-rich microwires. SEM was only used to image a single microwire as a representative sample to describe the general structure of these microwires including both their glass coating and their inner amorphous metal core.

2.3 Magnetic Measurements

The magnetic characterization of the microwires presented in this experiment was performed in a physical property measurement system (PPMS) from Quantum Design. The system can measure properties in a temperature range of 2 - 350 K and induce magnetic fields up to ± 7 Tesla [34]. The magnetic field in this wide temperature range is produced by a helium-cooled superconducting magnet. A vibrating sample magnetometer (VSM) was used to measure the magnetization (M) versus magnetic field (H) at 300 K and magnetization versus temperature (T) at 100 Oe in the temperature range between 5 K and 340 K [35].

The VSM magnetic measurements were done by placing a small sample of magnetic material in an external magnetizing field and measuring the magnetization of this sample by converting the dipole field of the sample into an AC electric signal, a principle stated in Faraday's law of induction. Measurements are made up to 2 cm from the sample to give space for temperature and pressure apparatuses. The voltage of the electrical signal is measured in terms of time rate of change of magnetic flux ϕ as described by the equation:

$$V_c = \frac{d\phi}{dt} = \frac{d\phi dz}{dzdt}$$

Where z is the vertical position of the sample with respect to the coil position. Once in the magnetic field, the sample is vibrated sinusoidally at an oscillation frequency f. The vibrations are usually conducted by a piezoelectric material or linear actuators. This creates a magnetic flux that passes through the pickup coil to induce the voltage V_c that is proportional to the sample's magnetic moment. This is not dependent on the strength of the field applied. The induced voltage is modeled by the following equation:

$$V_c = 2\pi CAfm \sin(2\pi ft)$$

Where C is the coupling constant, A is the amplitude of oscillation, and m is the DC magnetic moment of the sample. By measuring the field of an external electromagnet, a hysteresis curve of the material can be obtained. The magnetic hysteresis loops can then be analyzed to determine the sample's coercivity (H_c), saturation magnetization (M_s), and anisotropy field (H_k).

The coil used in this experiment with the Quantum Design PPMS is a standard gradiometer pickup coil with a pick-to-pick oscillation amplitude of 1-3 mm and a sample vibration of f = 40 Hz. It can resolve a change of 10^{-6} emu at a data rate of 1 Hz.

2.4 Magnetic Hyperthermia

In order to perform the hyperthermia experiments, the Co-rich microwires were cut into 5 mm strands. Multiple different configurations of microwire alloy, diameter, orientation, quantity, and separation were examined. The single microwire examinations were done for alloy number 1675 1-4 and 1597 7, 8, 10, 11, and 12. Alloy number 1675 1-4 were studied for their general differences in microwire diameter as both the core diameter and the glass thickness varied between the four samples. The samples from alloy number 1597 were carefully selected to investigate the effects of core diameter while the glass thickness was held constant and the

effects of the glass thickness while the core diameter was held constant. Alloy number 1597 7, 10, and 11 demonstrated the former effect while 1597-8 and 1597-12 demonstrated the latter effect. Additionally, the sample that demonstrated the best heating was used for additional experiments including orientation, i.e. horizontal versus vertical, and the effects of using multiple microwires.

The single microwire samples were prepared by inserting a single microwire 5 mm in length into a glass vial filled with 1 mL of deionized water. To test for orientation, the single microwire was placed into a 2% agar solution that would maintain the orientation of the microwire even under high magnetic fields. The orientation was imposed by the use of a small external permanent magnet and physically aligning it in solution before the agar cooled completely. Multiple microwire testing was done both in water and in agar. The tests in water would demonstrate natural microwire orientation in movement in a random distribution. On the other hand, the tests in agar were specifically done in different distributions or orientations, i.e. in situations where the wires are together, separated, and horizontal. The microwires in the multiple microwire experiments were also 5 mm in length.

In this experiment, we have used an Ambrell Easyheat system at the USF physics department that can generate an alternating magnetic field at a frequency between 150 – 400 kHz. Figure 2.2 shows an image of the water refrigerated multi-turn helical coil connected to a radio frequency power amplifier. Power to the system is provided by a generator. During the hyperthermia experiments, for each sample, the temperature evolution with time has been monitored while applying an external AC field, between 400 and 800 Oe, at a constant frequency of 310 kHz. The temperature was monitored by using a digital temperature probe which automatically recorded the data to the PC.

Figure 2.2 Magnetic hyperthermia system employed. Generator on the left and radio frequency amplifier on the right.

The heating efficiency, also known as the specific absorption rate (SAR), of the microwires has been estimated following calorimetric methods: the initial slope ΔT/Δt of the sample has been obtained from the measured curves, and the SAR values have been derived from the following formula:

$$SAR = C_p \cdot \frac{\Delta T}{\Delta t} \phi$$

where φ corresponds with the concentration of magnetic material, C_p is the heat capacity of water, and ΔT/Δt is the initial slope. The SAR measurements in agar were done in an identical way as it was assumed that the heat capacity change was negligible. To remove the heating contribution coming from the coil, we have subtracted the slope measured for the vial without sample from all our measurements. The initial slope was taken shortly after heating began but far before the sample reached temperature saturation, i.e. when the temperature increase was nearly linear.

Due to the small mass of these microwires (10^{-5} g), the final concentration value φ (0.01 mg/ml) is much smaller than those typically reported in the case of magnetic nanoparticles (0.5-5mg/ml). This is a big error source for the calculation of the SAR, and therefore, in those cases in which we are only working with 1 microwire, we have normalized the measurements to the maximum SAR value and just focused on the evolution of SAR as a function of the analyzed parameter (glass thickness, core diameter, wire alignment, etc.).

3. RESULTS AND DISCUSSION

This section consists of the results of the structural characterization methods of XRD and SEM, magnetic properties of all the microwires, and their effectiveness as hyperthermia agents. The tests include discussions of the effects of different variables including metallic core diameter, glass coating thickness, microwire number, separation, and orientation.

3.1 Structural Analysis

Figure 3.1 shows the XRD pattern for a single 5 mm sample of alloy number 1675-4.

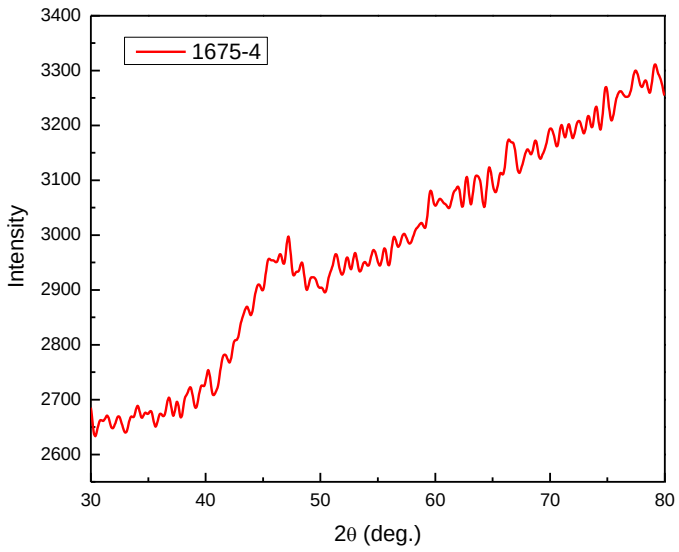

Figure 3.1 XRD pattern for glass-coated microwire 1675-4, i.e. $Co_{68}B_{15}Si_{10}Mn_7$ from 20° to 80°.

It can be observed that the XRD pattern exhibits only one broad peak around $2\theta = 45^0$, which is often known as a diffuse halo, indicating that the microwires prepared are amorphous in

nature. It has been reported that the amorphous magnetic microwires are more desirable for many applications due to their good mechanical properties as compared to their crystalline counterparts [25]. In our study, the microwires used are Co-based, so their particular magnetic domains are reserved if the wires are amorphous rather than crystalline.

3.2 Surface Morphology

Figure 3.2(a,b) shows the SEM images of a soft ferromagnetic amorphous glass-coated microwire for two different segments.

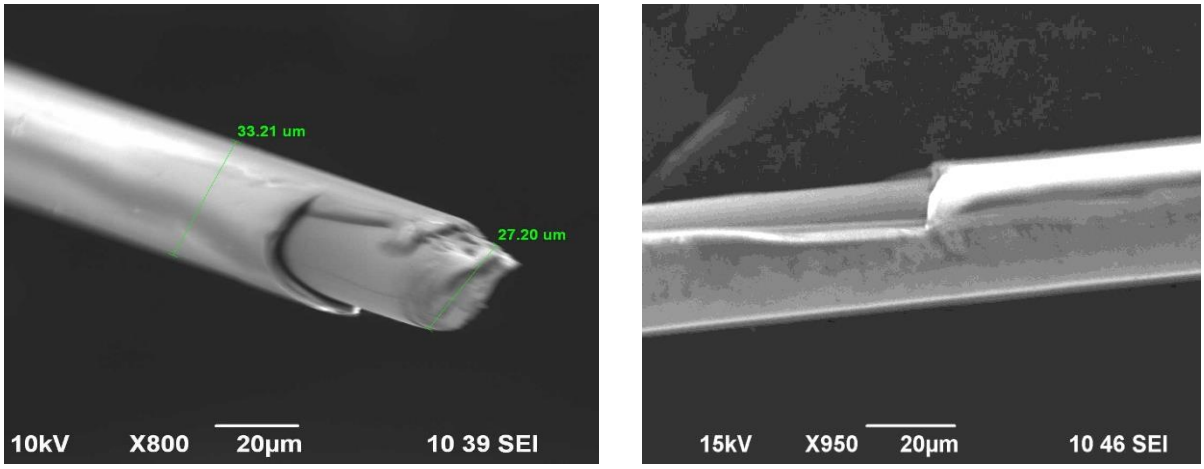

(a) (b)

Figure 3.2 SEM images of a glass-coated amorphous microwire 1675-4, i.e. $Co_{68}B_{15}Si_{10}Mn_7$ for two different segments (a,b).

The SEM images taken of 1675-4 are representative of all the glass-coated microwires used in this experiment. The average diameter of the metallic core and the average thickness of the glass layer can be determined from these images. It can be seen that the entire length of the microwire has a slightly variable diameter. While the surface of the glass coating layer is not very smooth, the surface of the metallic core is rather smooth. Therefore, we can expect these microwires to exhibit their good magnetic properties. Since the magnetic property of a microwire

depends sensitively on both the metallic core and the glass thickness, it is essential to investigate the effects of varying core diameter and glass thickness on the magnetic softness of the microwires studied in this thesis.

3.3 Magnetic Properties

The room temperature magnetic hysteresis M(H) loops were collected for all the microwires. The wires were then split into comparison views for the tests performed, i.e. the effects of differences in thickness of either the core as shown in Figure 3.3(a) or the glass coating as shown in Figure 3.3(b). It is generally observed that all microwires have negligible coercivity (H_c) and large saturation magnetization (M_s) indicative of their soft ferromagnetic characteristics. Upon closer inspection of the wires of comparative value, differences do begin to emerge about their M_s. As one can see clearly in Figure 3.3(a), 1675-4 has the largest M_s (~100 emu/g) and 1675-2 has the smallest M_s (~75 emu/g) among the four samples compared. This is attributed to the increased magnetic volume of the wire as the metallic core is increased while keeping the same glass thickness. The largest value of M_s suggests the best heating efficiency for the wire 1675-4.

Figure 3.3(b) shows the M(H) loops for the wires used in the comparison of the effect of glass thickness. Once again, there is a clear outlier for M_s as the wire 1579-11 is ~75 emu/g while neither 1579-7 nor 1579-10 is ~65 emu/g. This clearly demonstrates that for wires having the same diameter of the metallic core, the M_s is larger when the glass thickness is smaller. Since the heating efficiency is proportional to the M_s, one can expect significant effects of the metal core diameter and glass thickness on magnetic hyperthermia response.

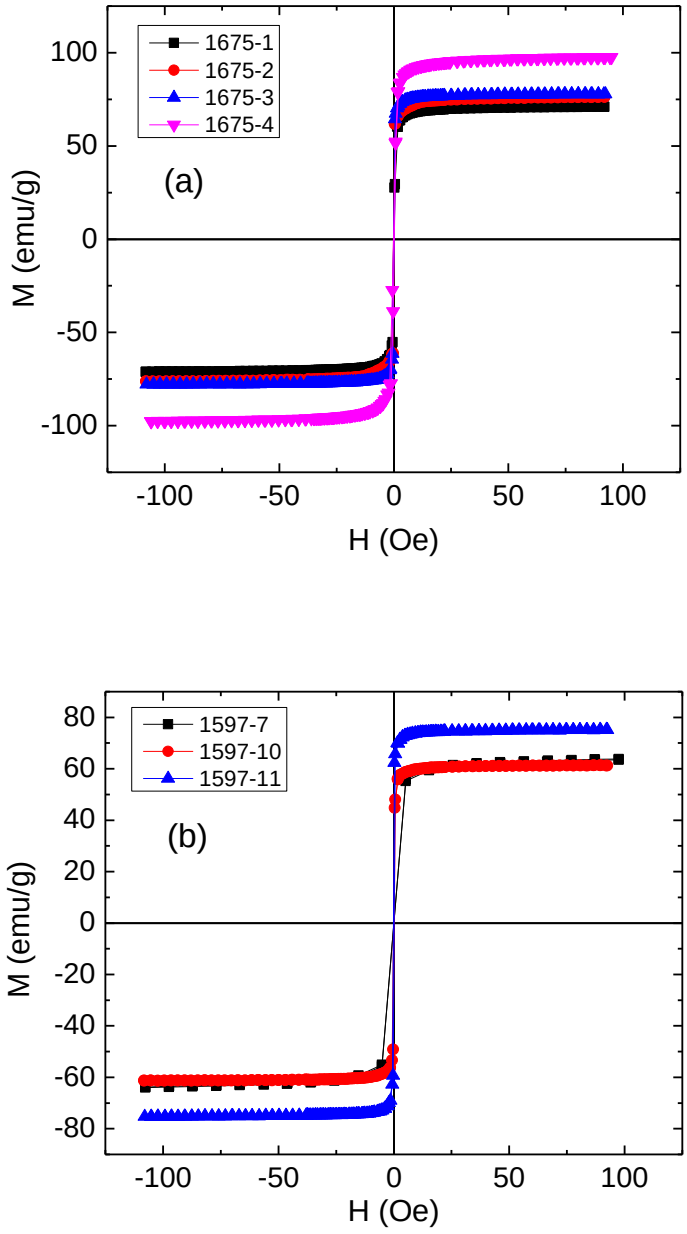

Figure 3.3 Room temperature magnetic hysteresis M(H) loops of the glass-coated amorphous microwires $Co_{68}B_{15}Si_{10}Mn_7$ and $Co_{64.63}B_{16}Si_{11}Fe_{4.97}Cr_{3.4}Ni_{0.02}$. (a) Hysteresis loops of only 1675-1, 2, 3, and 4 that vary by core diameter. (b) Loops of only 1597-7, 10, and 11 that vary only by glass thickness.

3.4 Magnetic Hyperthermia

These Co-rich amorphous microwires exhibit an appreciable heating efficiency. For example, in Fig 3.4(a) we have plotted the heating curves for 1 microwire, sample 1675-4, and as can be observed, the heating rate appreciably increases with increasing field.

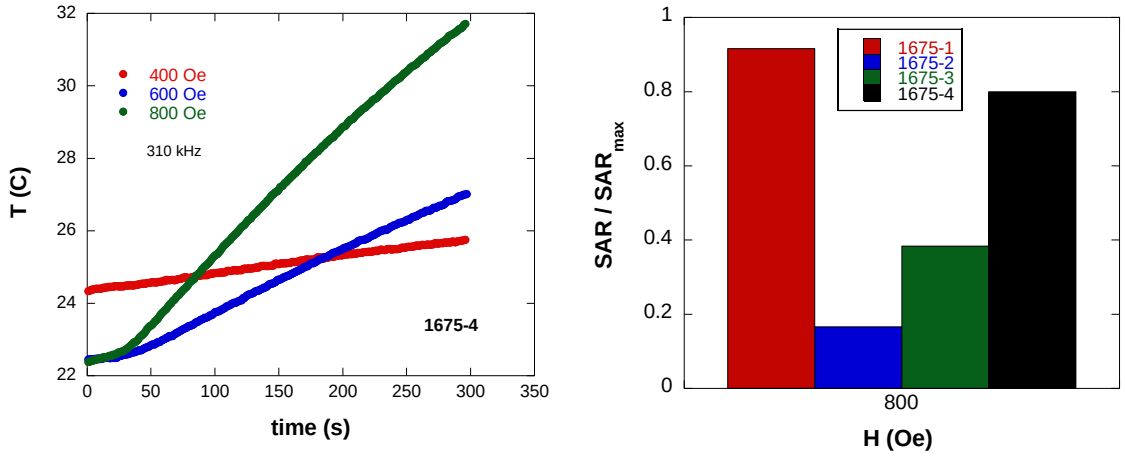

(a) (b)

Figure 3.4 (a) Temperature curves as a function of time at different fields (400-800 Oe) for sample 1675-4. (b) Normalized SAR values for 800 Oe for four samples of the same alloy (1675) with almost the same glass thickness and varying metal core diameters.

First, we have analyzed the overall effects of changes in microwire dimensions using four samples of the same alloy, 1675-1, 1675-2, 1675-3, and 1675-4. All the microwires are coated with glass, which acts as an insulating barrier and enhances the biocompatibility of these materials. In Figure 3.4(b) we have represented the SAR values for the four microwires that have almost the same glass thickness and varying metal core diameters. It can be observed that the SAR values of the samples 1675-1 and 1675-4 are much larger compared to the samples 1675-2 and 1675-3. In connection with the magnetization data, it is concluded that the 1675 wires with larger metal cores exhibit larger M_s and hence larger SAR. A similar trend has been observed for

the samples 1597-8 and 1597-12, with the same composition and the same glass thickness (~5.5 μm), but different core diameters, 12.7 and 14.2 μm, respectively. As observed in Fig 3.5(a,b), at 600 Oe, the thicker sample presents a better heating efficiency, but at higher fields, 800 Oe, the SAR values are similar, suggesting that at sufficiently high fields, the effect of the core diameter is less important than that at lower fields.

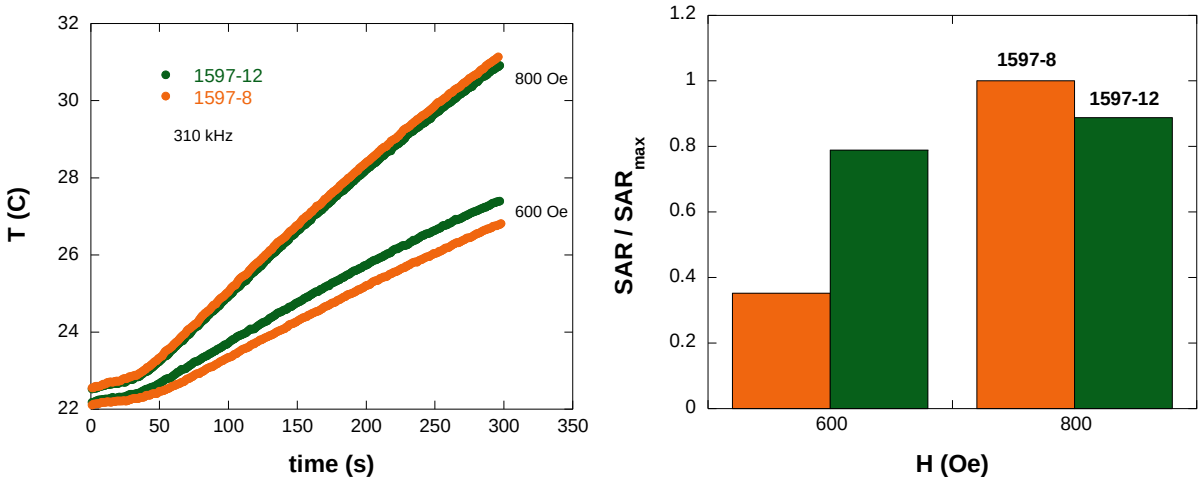

(a) (b)

Figure 3.5 Temperature curves and SAR values as a function of time at different fields (600 and 800 Oe) for samples with different core diameters.

Then, we have analyzed the effect of the glass thickness on the heating efficiency of these microwires. In Fig. 3.6(a,b) we have represented the heating curves for two samples, 1597-7 and 1597-10, with the same composition, the same diameter (~16.7 μm), but different glass thicknesses, 10 and 7 μm, respectively. As can be seen in this figure, with increasing glass thickness and increasing field the SAR values tend to decrease, indicating that the glass coating partially hinders the external heat transmission from the internal metallic core. Therefore, from the point of view of hyperthermia applications, the glass coating must be kept as thin as possible to enhance the heating efficiency of the microwires.

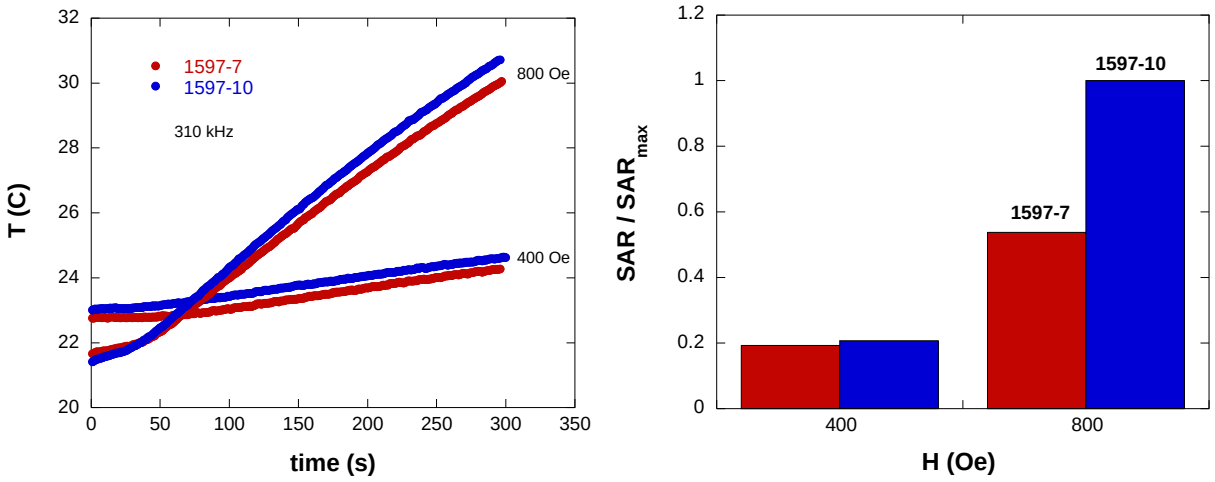

(a) (b)

Figure 3.6 Heating curves (a) and normalized SAR values (b) at different fields (400 and 800 Oe) for 1597 microwires with different glass thicknesses.

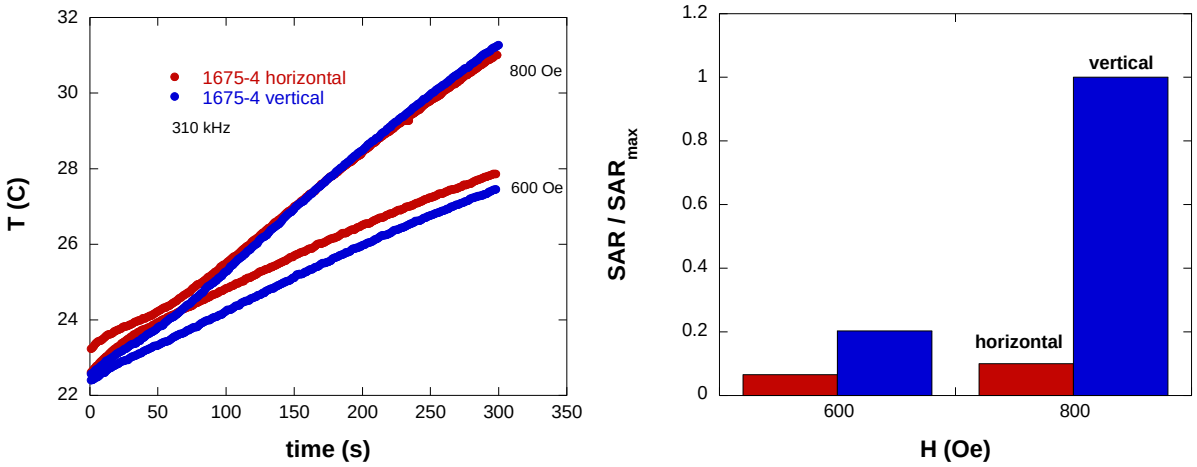

(a) (b)

Fig 3.7 Heating curves (a) and normalized SAR values (b) at different fields (600 and 800 Oe) for 1675-4 microwires with different alignments.

Next we have analyzed how the alignment of the wires affects the SAR values for the sample 1675-4. In order to carry out this study, we aligned the wires in agar, both in vertical (parallel to the field) and horizontal (perpendicular to the field) directions. The agar allows us to

fix the direction of the wire and make sure that the orientation does not change during the hyperthermia experiments. As observed in Fig 3.7, the heating efficiency is maximum when the wires are aligned in the direction of the field, and it greatly diminishes in the perpendicular direction. This is attributed to the strong shape anisotropy along the axis of the microwires.

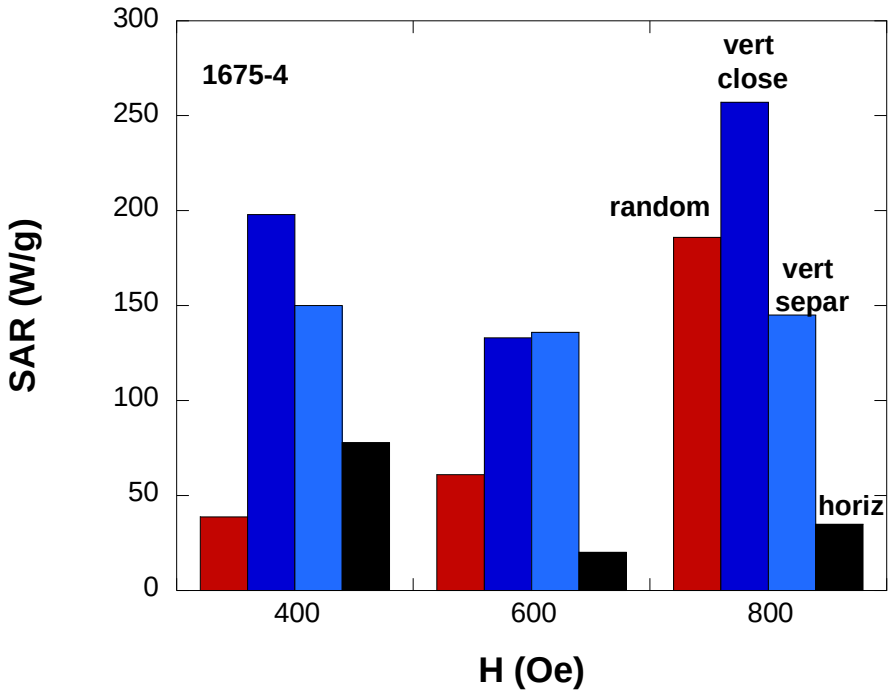

Fig 3.8 SAR values for the 1675-4 samples containing 5 microwires in different alignments.

Finally, we have measured the heating efficiency for multiple microwires (five), and compared how the SAR changes as a function of the orientation (vertical and horizontal) and as a function of the relative separation. In this case, the absolute values of SAR have been given since by increasing the number of wires, the previously commented error in the SAR determination appreciably diminishes. As can be seen in Fig. 3.8, the results indicate that when the wires are randomly pointing inside the water, their heating efficiency is lower than when they are all aligned in the field direction. In addition, it can also be observed that when the microwires are closer together the heating efficiency is higher than when they are separated.

4. CONCLUSIONS

4.1 Major Findings

Throughout this thesis, we have systematically demonstrated the potential of soft ferromagnetic glass-coated microwires for clinical hyperthermia applications. In particular, we have demonstrated appreciable heating rates of multiple microwires. We have also demonstrated conditions that permit glass-coated microwires to perform most efficiently based on size, thickness, orientation, and distribution to develop new glass-coated microwires that balance the best aspects from each of these studies. The important results from this thesis are summarized below:

We have investigated the use of glass-coated microwires as an alternative to magnetic nanoparticles. With their magnetic bistability, enhanced magnetic softness, large GMI effect, fast domain wall propagation, and Hopkinson effect, glass-coated microwires are a very promising alternative that does not require difficult and expensive synthesis techniques, possible biocompatibilities with some hosts, and toxic effects due to accumulation in body organs. Magnetization measurements demonstrated negligible coercivity (H_c ~ 0.2 Oe) high magnetization saturation (M_s ~ 100 emu/g) of the microwires. Additionally, we have demonstrated that single microwires show increasing heating efficiency with increased applied magnetic fields for both $Co_{64.63}B_{16}Si_{11}Fe_{4.97}Cr_{3.4}Ni_{0.02}$ and $Co_{68}B_{15}Si_{10}Mn_7$. Due to the small mass of these glass-coated microwires, however, their SAR values are only comparable to

nanoparticles when measuring multiple wires at a time. This way, the variance between each measurement of the microwire and the water has less possibility over overlapping resulting in imprecise data.

We have studied the effects of varying levels of glass-coating, varying from 6 to 10 μm in diameter, on hyperthermia efficiency of $Co_{64.63}B_{16}Si_{11}Fe_{4.97}Cr_{3.4}Ni_{0.02}$ microwires. As expected, increasing the external magnetic field from 400 to 800 Oe, the microwire with the thicker glass coat led to a decrease in SAR. 1597-7's higher SAR value demonstrates a more efficient release of heat than 1597-10. This provides some evidence that the glass coating does hinder the heat transfer between the metallic core and the surrounding environment. For biomedical applications, however, the glass-coat is important to retain the wires biocompatible. Further investigation must be done to determine the critical thickness that the glass-coat must be in order to maintain biocompatibility but still allow for efficient heat transfer. It is another controllable variable to continue to improve clinical hyperthermia optimization.

Further optimization can be accomplished by controlling the diameter of the metallic core. We have studied the influence of varying the metallic core diameter while retaining the same glass thickness in $Co_{64.63}B_{16}Si_{11}Fe_{4.97}Cr_{3.4}Ni_{0.02}$ microwires. As predicted, alloy number 1597-12, with its thicker metallic core, demonstrated higher SAR values at lower magnetic fields and approximately equal SAR values at higher magnetic fields. This indicates that a thicker microwire may be possible to implement at lower magnetic fields to achieve the same effect if higher magnetic fields are unavailable or are hazardous to the patient. Once again, however, a balance must be achieved because extremely thick microwires may result in rejection by the body, increase the difficulty in injecting the wires, or limit microwire movement to the target location.

We have also investigated the effects of orientation of the microwires, perpendicular and parallel, to the external field for both a single microwire and for a group of five microwires. Systematically, we have shown that the vertical orientation produces far better SAR values at all magnetic fields. This is the expected result based on the microwire's domain structure. With alternating circular domains perpendicular to the domain axis, these negative magnetostrictive alloys would perform best when the applied field was not interfering with the natural domain alignment. By acting in the axis of orientation, the external magnetic field is not impeded by the internal structure.

We have performed hyperthermia analysis for the use of multiple microwires in a single application in order to better replicate a real-world scenario. Because of the imprecision provided by the SAR values of single microwires, an understanding of how an increase in microwire count effects efficiency could not be achieved. Therefore, any data gained by measuring multiple microwires can only be compared with each other. With this in mind, we investigated the effects of controlling microwire distribution in solution. We have determined that the closer the microwires are, the better the heat loss. This combined efficiency was demonstrated to be better than a random separation and a controlled separation. The implications for biomedical implications are currently limited to the delivery technique used. However, it has been demonstrated that the induced dipole switching of one microwire does not negatively affect the heat loss of a nearby microwire.

Our study's goal was to explore and better understand the clinical hyperthermia applications of soft ferromagnetic glass-coated microwires, determine any biomedical implications for the results, and put the results into context for other magnetic particle treatments of hyperthermia. We have demonstrated that many of the properties of glass-coated microwires

do indeed make them ideal candidates for further investigation for clinical hyperthermia based on magnetization and structure. Additionally, we have revealed many characteristics that could be optimized to provide an even better heating efficiency than the wires used here. Finally, we have shown that these glass-coated microwires are very efficient at transferring heat homogenously to the external environment without interfering with each other. Based on these results, our hypothesis that the glass-coated microwires tested in this study would demonstrate highly efficient hyperthermia applications but only with proper orientation, glass thickness, and core diameter is supported.

4.2 Future Outlook

Having given a broad but limited study on the heating effects of amorphous soft ferromagnetic microwires, this thesis opens up innovative directions for further research into the hyperthermia applications of this class of microwire. Some examples are given below:

a. Our study provided insight into the difficulties in studying heat loss of single and small microwires. Therefore, future studies could limit their analysis to testing the same variables using single microwires with large magnetic cores (> 50 μm) or multiple microwires where the effects of error are decreased significantly. Those studies also can expand the use of multiple microwires from five to ten or more.

b. Proper studies on matching the real-life scenarios of clinical hyperthermia should be done with glass-coated microwires. In these tests, the microwires should be tested to investigate the time it takes to reach the clinical hyperthermia temperature range, how well the temperature can be maintained, and the distribution of heat between the target location and the surrounding environment/tissue. Different alloys, different glass-thicknesses, and different numbers of microwires could be tested.

c. While the Co-rich microwires were studied in this thesis, Fe-based microwires with appropriate compositions and dimensions could also be a competitive candidate for clinical hyperthermia applications. Suitable annealing of these Fe-based microwires could potentially improve their magnetic softness and hence inductive heating responses. Further research should thus be performed to exploit this class of microwires fully.

REFERENCES

[1] R. Alteri, T. Bertaut, D. Brooks and et al., "Cancer Facts & Figures 2015," American Cancer Society, Atlanta, 2015.

[2] B. Stewart and C. P. Wild, "World Cancer Report 2014," 2014.

[3] D. Ortega and Q. A. Pankhurst, "Magnetic hyperthermia," Nanoscience 1, 60 (2013).

[4] B. Chertok, B.A. Moffat, A.E. David, F.Q. Yu, C. Bergemann, B.D. Ross, V.C. Yang, Iron oxide nanoparticles as a drug delivery vehicle for MRI monitored magnetic targeting of brain tumors, Biomaterials 29, 487 (2008).

[5] M. Colombo, S. Carregal-Romero, M.F. Casula, L. Gutierrez, M.P. Morales, I.B. Bohm, J.T. Haverhagen, D. Prosperi, W.J. Parak, Biological applications of magnetic nanoparticles, Chemical Society Reviews 41, 4306 (2012).

[6] Q.A. Pankhurst, J. Connolly, S.K. Jones, J. Dobson, Applications of magnetic nanoparticles in biomedicine, Journal of Physics D: Applied Physics 36, R167 (2003).

[7] E. A. Skyes, Q. Dai, K. M. Tsoi, D. M. Hwang and W. C. W. Chan, "Nanoparticle exposure in animals can be visualized in the skin and analyzed via skin biopsy," Nature Communications 5, 3796 (2013).

[8] P.R. Stauffer, T. C. Cetas, A.M. Flectcher, D. W. DeYoung, M. E. DeWhirst, J. R. Oleson, and R. B. Roemer, “Observations on the use of ferromagnetic implants for inducing hyperthermia.” IEEE Trans. Biomed. Eng. 31, 76 (1984).

[9] R. Zuchini, H.-W. Tsai, C.-Y. Chen, C.-H. Huang, S.-C. Huang, G.-B. Lee, C.-F. Huang, and X.-Z. Lin, Electromagnetic thermotherapy using fine needles for hepatoma treatment. Eur. J. Surg. Oncol. 37, 604 (2011).

[10] R. Hudak, R. Varga, J. Hudak and D. Praslicka, "Influence of Fixation on Magnetic Properties of Glass-Coated Magnetic Microwires for Biomedical Applications," IEEE Transactions on Magnetics 51, 5200104 (2015).

[11] M. Vázquez, “Soft magnetic wires,” Physica B 299, 302 (2001).

[12] M. Banobre-Lopeez, A. Teijeiro, and J. Rivas, “Magnetic nanoparticle-based hyperthermia for cancer treatment,” Reports of Practical Oncology and Radiotherapy 18, 397 (2013).

[13] A. Jordan, P. Wust, H. Fahling, W. John, A. Hinz, R. Felix, Inductive Heating of Ferrimagnetic Particles and Magnetic Fluids - Physical Evaluation of Their Potential for Hyperthermia, International Journal of Hyperthermia 9, 51 (1993).

[14] R. K. Gilchrist, W. D. Shorey, R. C. Hanselman, F. A. DePeyster, J. Yang, and R. Medal, “Effects of Electromagnetic Heating on Internal Viscera: A Preliminary to the Treatment of Human Tumors,” Annals of Surgery 161, 890 (1965).

[15] O. Lucia, "Induction Heating and Its Applications: Past Developments, Current Technology, and Future Challenges," Transactions on Industrial Electronics 61, 2509 (2014).

[16] A. Figuerola, R. Di Corato, L. Manna, T. Pellegrino, From iron oxide nanoparticles towards advanced iron-based inorganic materials designed for biomedical applications, Pharmacological Research 62, 126 (2010).

[17] C. G.-P. e. al, "Magnetic induction heating of FeCr nanocrystalline alloys," Journal of Magnetism and Magnetic Materials 324, 1897 (2012).

[18] C. Gomez-Polo, S. Larumbe, J. I. P.-. Landazabal and J. M. Pastor, "Analysis of heating effects (magnetic hyperthermia) in FeCrSiBCuNb amorphous and nanocrystalline wires," Journal of Applied Physics 111, 07A314 (2012).

[19] H. Mamiya and B. Jeyadevan, "Magnetic Hysteresis Loop in a Superparamagnetic State," IEEE Transactions on Magnetics 50, 4001604 (2014).

[20] G. C. Papaefthymiou, “Nanoparticle magnetism,” Nano Today 4, 438 (2009).

[21] A. H. Lu, E. L. Salabas, and F. Schuth, Anegewandte Chemie-International Edition, vol. 46, 2007.

[22] Y.W. Jun, J.W. Seo, A. Cheon, “Nanoscaling laws of magnetic nanoparticles and their applicabilities in biomedical sciences,” Accounts of Chemical Research 41, 179 (2008).

[23] R. Varga, “Magnetization Processes in Glass-Coated Microwires with Positive Magnetostriction,” Acta Physica Slovaca 62, 411 (2012).

[24] A. Jordan, P. Wust, H. Fahling, W. John, A. Hinz, R. Felix, Inductive Heating of Ferrimagnetic Particles and Magnetic Fluids - Physical Evaluation of Their Potential for Hyperthermia, International Journal of Hyperthermia 9, 51 (1993).

[25] M. H. Phan and H. X. Peng, “Giant magnetoimpedance materials: Fundamentals and applications,” Progress in Materials Science 53, 323 (2008).

[26] J.P. Sinnecker, J.M. Garcia, A. Asenjo, M. Vazquez, A. Garcia-Arribas, “Giant magnetoimpedance in CoP electrodeposited microtubes,”. J Mater Res 15, 751 (2000).

[27] P. Jantaratana, C. Sirisathitkul, “Effects of thickness and heat treatments on giant magnetoimpedance of electrodeposited cobalt on silver wires,” IEEE Trans Magn 42, 358 (2006).

[28] G. F. Taylor, “A method of Drawing Metallic Filaments and Discussion of Their Properties and Uses,” Phys Rev 23, 655 (1924).

[29] Taylor GF. Process and apparatus for making filaments, Patented February 24, 1931, United States Patent Office, 1, 793, 529.

[30] A. V. Ulitovsky, Leningrad, vol. 7, pp. 6, 1951.

[31] H. Wiesner and Schneider, “Magnetic Properties of amorphous FeP alloys containing Ga, Ge, and As,” Physica Status Solidi 29, 71 (1974).

[32] H. P. Klug and L. E. Alexander, X-ray diffraction procedures for polycrystalline and amorphous materials, New York: Wiley, 1974.

[33] J. Goldstein, Scanning electron microscopy and x-ray microanalysis, Kluwer Adacemic/Plenum Pulbishers, 2003

[34] "Physical Property Measurement System (PPMS®)," Quantum Design, [Online]. Available: http://www.qdusa.com/products/ppms.html.

[35] D. O. Smith, "Development of a Vibrating-Coil Magnetometer," Review of Scientific Instruments 27, 261 (1956).